Electronic structure and orbital polarization of LaNiO_{3} with a reduced coordination and under strain: A first-principles study

Myung Joon Han and Michel van Veenendaal

Phys. Rev. B **84**, 125137 — Published 29 September 2011

DOI: 10.1103/PhysRevB.84.125137

Electronic structure and orbital polarization of $LaNiO_3$ with a reduced coordination and under strain: first-principles study

Myung Joon Han and Michel van Veenendaal
Department of Physics, Northern Illinois University, De Kalb, Illinois 60115, USA and
Advanced Photon Source, Argonne National Laboratory,
9700 South Cass Avenue, Argonne, Illinois 60439, USA
(Dated: August 18, 2011)

First-principles density functional theory calculations have been performed to understand the electronic structure and orbital polarization of $LaNiO_3$ with a reduced coordination and under strain. From the slab calculation to simulate [001] surface, it is found that $d_{3z^2-r^2}$ orbital occupation is significantly enhanced relative to $d_{x^2-y^2}$ occupation owing to the reduced coordination along the perpendicular direction to the sample plane. Furthermore, the sign of the orbital polarization does not change under external strain. The results are discussed in comparison to the bulk and heterostructure cases, which sheds new light on the understanding of the available experimental data.

PACS numbers: 73.20.-r, 75.70.-i, 71.15.Mb

I. INTRODUCTION

Understanding transition metal oxides is of perpetual interest and importance in condensed matter physics and material science due to their great scientific and technological potential[1]. Recent advances in layer-by-layer growth techniques of these compounds in the form of thin film and heterostructures have created considerable interest and enabled a further understanding of these systems[2]. Exotic material phenomena that are clearly distinctive from the 'normal' phases include interface superconductivity[3], charge[4,5] and orbital reconstruction[6], and room-temperature ferromagnetism[7]. Strain-mediated[8] and electric field control[9] of the metal-insulator phase transition are the other examples of thin-film phenomena.

One of the most interesting classes of transition-metal oxide systems is thin film $LaNiO_3$ (LNO) and heterostructures of LNO and wide-gap insulators such as $LaAlO_3$ (LAO). Bulk LNO is the only member in the $ReNiO_3$ series (*Re*: La, Pr, Nd,...*etc.*) that remains metallic at all temperatures[1,10]. As a result, thin film LNO and LNO-based heterostructures have been studied under various strained conditions to control the correlation strength and the metal-insulator phase transition[11–14] in an effort to find possible high temperature superconductivity[15] and conductivity enhancement[16]. Strain affects most strongly the orbital character of the nickelates[15,17–20]. Recently, several papers have focused on how changes in orbital polarization in heterostructures and thin films affect the electronic structure and thereby the macroscopic material properties[15,17–22].

An important issue is the relationship between strain and the orbital polarization in various structural classes of nickelates. For low-spin trivalent nickelates, the orbital polarization P can be defined simply as the difference of the two e_g orbital occupations (without renormalization factor)

$$P = n_{x^2-y^2} - n_{3z^2-r^2}. \quad (1)$$

By definition, a positive orbital polarization indicates a higher electron occupation in the $d_{x^2-y^2}$ orbital compared to the $d_{3z^2-r^2}$ state. Recent x-ray linear dichroism (XLD) measurements on nickelate superlattices and thin films have reported intriguing behavior of the orbital polarization P under strain. Beside the transformation into a different structural phase[17], the polarization change under compressive and tensile strain has mainly been analyzed using Madelung energies. However, the detailed changes in electronic structure cannot be understood from such a simple electrostatic approach[17,18]. For example, both in film and in heterostructures of LNO, compressive strain make the $d_{3z^2-r^2}$ orbital more occupied, as one would expect. However, tensile strain does not make the polarization go the other way which is in a clear contradiction to Madelung picture.

In this paper, we investigate the electronic structure and orbital occupation by using first-principles density functional theory (DFT) calculations. Special attention has been paid to the surface Ni state as its contribution might be significant in thin film and in surface-sensitive measurements. The electronic structure and orbital property are compared to the results of heterostructure and bulk counterpart. Translational symmetry breaking along the direction perpendicular to the sample and the reduced coordination at the surface are found to strongly change the orbital polarization with respect to the bulk. The effects of strain are also studied. Our results shed new light on understanding the available experimental data.

II. COMPUTATIONAL DETAILS

For the band-structure calculations, we employed Troullier-Martins type norm-conserving

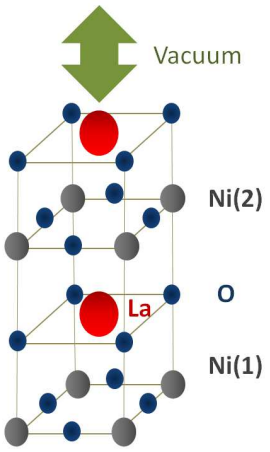

FIG. 1: (Color online) Unitcell structure of the double layer slab calculation. Large (red), middle (gray), and small (blue) size spheres represent La, Ni, and O atoms, respectively. Ni(1) and Ni(2) corresponds to the surface-like and bulk-like Ni sites respectively.

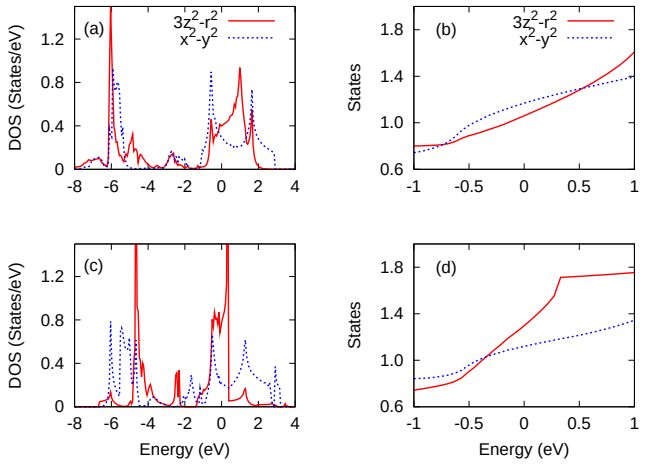

FIG. 2: (Color online) (a) Projected DOS and (b) integrated DOS of Ni e_g states in $(LNO)_1/(LAO)_1$ heterostructure. (c) Projected DOS and (d) integrated DOS of Ni e_g states in single layer LNO slab. Red (solid) and blue (dashed) lines correspond to $d_{3z^2-r^2}$ and $d_{x^2-y^2}$ states, respectively. The Fermi level is set to be zero.

pseudopotential[23] with a partial core correction and linear-combination-of-localized-pseudo-atomic orbitals (LCPAO)[24] as a basis set. In this pseudo-potential generation, the semi-core $3p$ electrons for transition metal atoms were included as valence electrons in order to take into account the contribution of the semi-core states to the electronic structures. Basis orbitals are generated by a confinement potential scheme[24] with the cutoff radius 7.0 a.u., 5.5 a.u., and 5.0 a.u. for La, Ni, and O, respectively. We adopted the local density approximation (LDA) for exchange-correlation energy functional as parametrized by Perdew and Zunger[25], and used energy cutoff of 400 Ry and k-grid of $10 \times 10 \times 10$. All the DFT calculations were performed using the DFT code OpenMX[26].

To simulate the [001] surface, the single and double layered slab geometries have been investigated. The unitcell structure for the double layer slab is presented in Fig. 1. This is thinner than what is commonly used experimentally, but it allows us to obtain a better understanding of the surface effects. Vacuum layer thickness is of 7.0 Å which is large enough to make the basis function overlap negligible. While the polar surface may not be well stabilized in general, these instability can be compensated by the large covalency in the nickelates[11,12,17,18]. The geometry relaxation has been performed with the force criterion of 10^{-3} Hartree/Bohr. During the relaxation process, the in-plane lattice constant is fixed considering the substrate effect in the experimental situation. The presence of vacuum layer naturally allows the atomic movement along the out-of-plane axis and the volume change. We considered the paramagnetic phase because the bulk LNO is paramagnetic metal and there is no report on the magnetic ordering in the thin film LNO. The orbital polarization P can be calculated by integrating the projected density-of-states (DOS) up to Fermi level. For the atomic charge density we used Mulliken analysis based on the generated pseodo-atomic basis orbitals[24,26].

III. RESULT AND DISCUSSION

In an ideal cubic structure of LNO, Ni^{3+} ion has (formally) singly occupied degenerate e_g orbitals around the Fermi level. This degeneracy can be lifted by, for example, making a heterostructure with a LAO interlayer[15]. It has also been noted that the e_g orbitals in LNO/LXO (X=B, Al, Ga, In) superlattice are positively polarized without strain[19]. The positive polarization is attributed to the reduced hybridization along the z-direction (perpendicular to the sample plane) due to the presence of the LAO layers. As a result, the width of the bands with strong $d_{3z^2-r^2}$ character is smaller compared to $d_{x^2-y^2}$. The wider $d_{x^2-y^2}$-related bands are more occupied than the narrower $d_{3z^2-r^2}$ band. The calculated e_g orbital DOS for $(LNO)_1/(LAO)_1$ heterostructure is presented in Fig. 2(a). Fig. 2(b), the integrated DOS of Fig. 2(a), clearly shows that $d_{x^2-y^2}$ orbital is more occupied than $d_{3z^2-r^2}$. Note that the orbital polarization is present in the absence of strain.

For a surface, the symmetry is also broken along the z-direction, but, in addition, the Ni coordination is reduced. The calculated e_g DOS of the single layer slab is shown in Fig. 2(c). First, the band width of the $d_{3z^2-r^2}$ states is less than 2 eV which is not only significantly smaller than the bulk value of $\sim$ 4.5 eV, but also reduced compared to the LNO/LAO heterostructure where the band width is larger than $\sim$ 2 eV. On the other hand, the width of the $d_{x^2-y^2}$-related bands remains comparable to the bulk value. For the heterostructure, the nar-

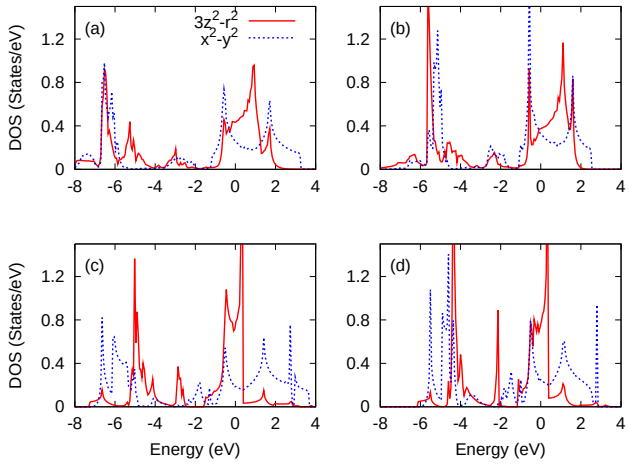

FIG. 3: (Color online) Projected DOS for Ni e_g states in a LNO/LAO heterostructure ((a) and (b)), and single layer slab ((c) and (d)). (a) and (c) are calculated under compressive strain (−3% in-plane lattice mismatch), and (b) and (d) under tensile strain (+3% in-plane lattice mismatch). Red (solid) and blue (dashed) lines correspond to $d_{3z^2-r^2}$ and $d_{x^2-y^2}$ states, respectively. The Fermi level is set to be zero.

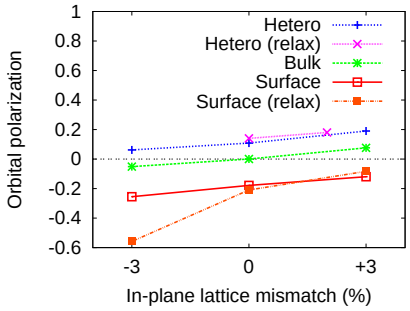

FIG. 4: (Color online) Calculated orbital polarizations for a LNO/LAO heterostructure (blue), bulk LNO (green), and unrelaxed (red) and relaxed slab (orange) as a function of strain. Horizontal dotted line shows the zero polarization points. The relaxed result for heterostructure (magenta) is from Ref.[19] with re-normalization.

rower $d_{3z^2-r^2}$ band is located roughly in the middle of the $d_{x^2-y^2}$ band, and the Fermi level is slightly below the middle point of the two bands, and the $d_{x^2-y^2}$ orbital is therefore more occupied than the $d_{3z^2-r^2}$ (Fig. 2(a)). As a result, positive orbital polarization is induced as is clearly seen in Fig. 2(b). In the surface Ni site, on the other hand, the energy level of the $d_{3z^2-r^2}$ state comes down to the bottom of $d_{x^2-y^2}$ band due to the change in nickel coordination and the Fermi level is roughly at the middle of $d_{3z^2-r^2}$ state (Fig. 2(c)). As a result, $d_{3z^2-r^2}$ orbital is more occupied than $d_{x^2-y^2}$. This corresponds to a negative orbital polarization, see Fig. 2(d). Again, this negative orbital polarization at the surface Ni state is a direct result of its local geometry and present without any additional strain effects.

Let us now turn our attention to the effects of the strain. We took the relaxed LNO cubic bulk lattice parameter (~ 3.81 Å) as a reference, and applied compressive and tensile strain by setting the in-plane lattice parameter to be smaller and larger, respectively. The ±3% of strain considered here is in a reasonable range to simulate the experimental situation. For example, LAO, a widely used substrate for the compressive strain, has a lattice parameter of 3.78 Å, and $SrTiO_3$, a popular substrate material for compressive strain, has 3.91 Å.

Fig. 3(a) and (b) shows Ni DOS in the heterostructure under compressive (−3%) and tensile (+3%) strain, respectively. Similarly, Fig. 3(c) and (d) represents surface Ni DOS for −3% and +3% strain, respectively. The strain shifts the relative energy positions of the bands. However, the changes in orbital occupation are small and no sign reversal in the orbital polarization is found. The calculated polarization of the compressive and tensile strained heterostructure is 0.06 (Fig. 3(a)) and 0.19 (Fig. 3(b)), respectively, and the polarization of surface is −0.25 (Fig. 3(c)) for compressive case and −0.12 for tensile (Fig. 3(d)).

The results of the changes in orbital polarization are summarized as a function of strain in Fig. 4. For bulk LNO, the two e_g orbital states are degenerate under the cubic symmetry, and strain plays the major role in determining the sign of orbital polarization. Under the −3% of compressive strain, $d_{3z^2-r^2}$ orbital is more occupied leading to negative orbital polarization, and the compressive strain results in the positively polarized orbital occupation. Therefore the simple electrostatic picture works well in the bulk case. For heterostructures and surfaces, however, the symmetry breaking leads those systems to have asymmetric electronic structures and orbital occupations even without any strain as discussed in the above. The lattice strain is playing its role on top of the modified electronic structures, and does not change the sign of polarization within the range of ±3% lattice mismatch. As is clearly seen in Fig. 4, in the heterostructure, Ni orbitals are positively polarized and remain positive down to −3% strain. In the surface case, the negatively polarized orbital states is retained up to +3%.

Rearrangements of atomic positions at the surface often play an important role and cause a significant change in the electronic structure. It is therefore important to check the relaxation-induced change of the electronic structure and orbital occupation. From the force minimization calculations, it is found that the basic features of the electronic structure and orbital polarization at the surface do not change even after the relaxation. We performed the calculations within the three different in-plane lattice parameters corresponding to the compressive, zero and tensile strain, and the result of the calculated orbital polarizations are presented in Fig. 4 (dashed-dotted line with filled square boxes) from which one can see some deviation of the polarization trend but the basic feature is retained. Ionic movements make polarization slightly smaller and larger under the zero and +3% strain, respectively, with respect to the unrelaxed results

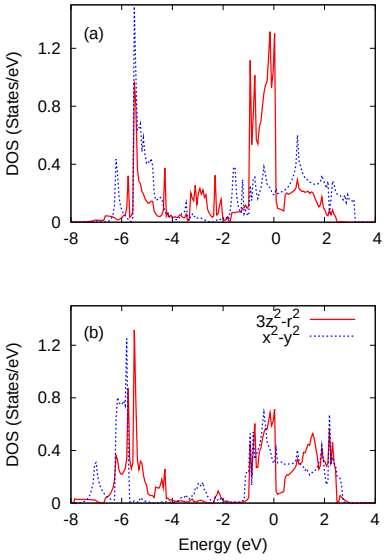

FIG. 5: (Color online) Projected Ni-e_g DOS in the double layer slab structure. (a) represents to the top layer Ni site that has only five neighboring oxygens, and (b) shows the second layer Ni site that has six neighbors. Red (solid) and blue (dashed) lines correspond to $d_{3z^2-r^2}$ and $d_{x^2-y^2}$ states, respectively, and Fermi level is set to be zero.

(solid red line with open boxes). It is found that the relaxation-induced change becomes much larger in the compressively strained situation, which is attributed to the large ionic displacement along the out-of-plane direction caused by the compressive in-plane strain, and the volume conservation often being observed in the related materials[12,18]. In the zero strain case, the optimized distance between Ni and apical oxygen is $\sim$ 2.04 Å . It is decreased by 4% under the tensile strain and increased by 11% under the compressive strain. La ions also moved slightly in response to strains; toward and out-of the NiO_2 plane by 0.04 and 0.09 Å in case of tensile and compressive strain, respectively. In-plane oxygens (in the NiO_2 plane) are found to move toward LaO plane by 0.06 Å in case of compressive strain while it stays at almost same position under tensile strain. It should be noted that the calculated ionic movements is from the very thin slab calculation. In realistic situation in which the film thickness is much larger ($\geq 10\ nm$) and it is on the substrate, the induced polarization change is much smaller and therefore is closer to the unrelaxed result (Fig. 4).

Another important issue regarding the surface is the thickness of surface-like layers. To understand this point, we performed two-layer slab calculation. In this structure, the first layer Ni ion (*i.e.,* Ni(1) in Fig. 1) has the reduced coordination, and the second layer Ni site (*i.e.,* Ni(2) in Fig. 1) has the octahedron oxygen environment as in the bulk. As shown in Fig. 5(b), the cubic symmetry is significantly restored at the second-layer Ni site and the two e_g states become bulk-like. The difference in the two e_g orbital occupation is actually small, and the calculated orbital polarization is -0.02. The small deviation between $d_{3z^2-r^2}$ and $d_{x^2-y^2}$ is the proximity to the surface state. The first layer Ni is similar to the single layer case (Fig. 5(a)), the polarization of which is -0.42. In addition, it is noted that the $d_{3z^2-r^2}$ DOS at the Fermi level is reduced in Ni(2). Large DOS in Ni(1) as also observed in single-layer case may indicate the possible unstability of the surface and the other reactions such as chemisorptions or stoichiometric changes.

Our results shed new light on the interpretation of recent experiments. It is found from XLD measurement that compressively strained LNO thin film has negative orbital polarization whereas the tensile strain does not produce the sign reversal in the polarization[17], which is in a contradiction to the simple electrostatic Madelung picture assuming the same energy levels both for $d_{x^2-y^2}$ and $d_{3z^2-r^2}$ [17]. Our calculation provides a natural explanation as a surface effect dominant situation; *i.e.,* the electronic structure change mainly caused by the reduced coordination is responsible for the negative polarization, and the effect persists even under the tensile strain. The case of heterostructure is more delicate especially because the XLD shows no orbital polarization in the tensile strain case for which the simple electrostatic theory predicts the positive orbital polarization. According to our calculations, the tensile strain should enhance the positive orbital polarization in heterostructure. The observation can be understood if there is some contribution from surface-like states even for the heterostructure case. As the $d_{x^2-y^2}$ orbital is preferred in the heterostructure while $d_{3z^2-r^2}$ is at the surface, there can be a compensation between the two which may result in the negligible polarization along with the relatively small effect from the strains.

IV. SUMMARY

In conclusion, using density-functional theory, we have shown the change in the electronic structure of nickelates as a function of reduced dimensionality and strain. In surface Ni, the reduction of the coordination leads to a significant local crystal field. This leads to a negative orbital polarization both in the absence and presence of strain effects. It is notably different from the positive orbital polarization found in heterostructures where the asymmetric DOS caused by the strongly reduced hybridization along the out-of-plane direction results in a higher electron occupation of the x^2-y^2 orbitals. Strain is found to play a relatively minor role on top of the modified electronic structure of each system, and the sign of polarization does not change under the moderate strains. Our results are providing new insights for understanding recent experiments on the related systems.

V. ACKNOWLEDGMENTS

We thank Jak Chakhalian, Jian Liu, and John Freeland for useful discussion. This work was supported by the U.S. Department of Energy (DOE), DE-FG02-03ER46097, and NIUs Institute for Nanoscience, Engineering, and Technology. Work at Argonne National Laboratory was supported by the U.S. DOE, Office of Science, Office of Basic Energy Sciences, under Contract No. DE-AC02-06CH11357.

[1] M. Imada, A. Fujimori, and Y. Tokura, Rev. Mod. Phys. **70**, 1039 (1998).
[2] For a reveiw, see, J. Mannhart, D. H. A. Blank, H. Y. Hwang, A. J. Millis, and J. M. Triscone, Bulletin of the Materials Research Society **33**, 1027 (2008).
[3] N. Reyren, S. Thiel, A. D. Caviglia, L. F. Kourkoutis, G. Hammerl, C. Richter, C. W. Schneider, T. Kopp, A.-S. Rüetschi, D. Jaccard, M. Gabay, D. A. Muller, J.-M. Triscone, J. Mannhart, Science **317**, 1196 (2007).
[4] A. Ohtomo, D. A. Muller, J. L. Grazul, and H. Y. Hwang, Nature **419**, 378 (2002).
[5] S. Okamoto and A. J. Millis, Nature **428**, 630 (2004).
[6] J. Chakhalian, J. W. Freeland, H.-U. Habermeier, G. Cristiani, G. Khaliullin, M. van Veenendaal, and B. Keimer, Science **318**, 1114 (2007).
[7] U. Lüders, W. C. Sheets, A. David, W. Prellier, and R. Frésard, Phys. Rev. B **80**, 241102 (2009).
[8] J. Liu, M. Kareev, B. Gray, J. W. Kim, P. Ryan, B. Dabrowski, J. W. Freeland, and J. Chakhalian, Appl. Phys. Lett. **96**, 233110 (2010).
[9] R. Scherwitzl, P. Zubko, I. G. Lezama, S. Ono, A. F. Morpurgo, G. Catalan, and J.-M. Triscone, Adv. Mater. **22**, 5517 (2010).
[10] J. B. Torrance, P. Lacorre, A. I. Nazzal, E. J. Ansaldo, and C. Niedermayer, Phys. Rev. B **45**, 8209 (1992).
[11] D. G. Ouellette, S. B. Lee, J. Son, S. Stemmer, L. Balents, A. J. Millis, and S. J. Allen, Phys. Rev. B **82**, 165112 (2010).
[12] M. K. Stewart, C.-H. Yee, J. Liu, M. Kareev, R. K. Smith, B. C. Chapler, M. Varela, P. J. Ryan, K. Haule, J. Chakhalian, and D. N. Basov, Phys. Rev. B. **83** 075125, (2011).
[13] J. Liu, S. Okamoto, M. van Veenendaal, M. Kareev, B. Gray, P. Ryan, J. W. Freeland, and J. Chakhalian, Phys. Rev. B. **83** 161102, (2011).
[14] A. V. Boris, Y. Matiks, E. Benckiser, A. Frano, P. Popovich, V. Hinkov, P. Wochner, M. Castro-Colin, E. Detemple, V. K. Malik, C. Bernhard, T. Prokscha, A. Suter, Z. Salman, E. Morenzoni, G. Cristiani, H.-U. Habermeier, and B. Keimer, Science **332**, 937 (2011).
[15] P. Hansmann, X. Yang, A. Toschi, G. Khaliullin, O. K. Andersen, and K. Held, Phys. Rev. Lett. **103**, 016401 (2009).
[16] J. Son, J. M. LeBeau, S. J. Allen, and S. Stemmer, Appl. Phys. Lett. **97**, 202109 (2010).
[17] J. Chakhalian, J.M. Rondinelli, J. Liu, B. Gray, M. Kareev, E. J. Moon, M. Varela, S. G. Altendorf, F. Strigari, B. Dabrowski, L.H. Tjeng, P.J. Ryan, and J. W. Freeland, arXiv:1008.1373 (2010).
[18] J. W. Freeland, J. Liu, M. Kareev, B. Gray, J.W. Kim, P. Ryan, R. Pentcheva, and J. Chakhalian, arXiv:1008.1518 (2010).
[19] M. J. Han, C. A. Marianetti, and A. J. Millis, Phys. Rev. B. **82** 134408, (2010).
[20] M. J. Han, X. Wang, C. A. Marianetti, and A. J. Millis, arXiv:1105.0016 (2011).
[21] S. J. May, T. S. Santos, and A. Bhattacharya, Phys. Rev. B **79** 115127, (2009).
[22] S. J. May, J.-W. Kim, J. M. Rondinelli, E. Karapetrova, N. A. Spaldin, A. Bhattacharya, P. J. Ryan, Phys. Rev. B **82** 014110, (2010).
[23] N. Troullier and J. L. Martins, Phys. Rev. B **43**, 1993 (1991).
[24] T. Ozaki, Phys. Rev. B. **67**, 155108, (2003); T. Ozaki and H. Kino, Phys. Rev. B **69**, 195113, (2004); T. Ozaki and H. Kino, J. Chem. Phys. **121**, 10879, (2004).
[25] D. M. Ceperley and B. J. Alder, Phys. Rev. Lett. **45**, 566(1980); J. P. Perdew and A. Zunger, Phys. Rev. B **23**, 5048 (1981).
[26] http://openmx-square.org